METHODOLOGY TO EVALUATE VIBRATION INCREASE DUE TO THERMAL ROTOR BOW – A COMPARISON BETWEEN ALUMINUM AND COPPER CAGES USED IN INDUCTION MOTORS

Ribeiro Neto, Rubem
GEVISA S/A Rod. SP-101, km 3,8 CEP 13064-654 Campinas – SP Brazil
rubem.ribeiro@ge.com; rubem_neto@uol.com.br

Oliveira Jr., Silvio
Escola Politécnica da USP – Departamento de Engenharia Mecânica Av. Prof. Mello Soares, 2231 Sala TS 13 Cidade Universitária Armando de Salles CEP 05508-900 São Paulo – SP Brazil
silvio.oliveira@poli.usp.br

Abstract. A methodology to evaluate the root causes of vibration increase in rotary machinery as function of temperature change and/or uneven deformation of rotor parts is proposed. Using a finite element model of the rotor and linear static analysis, the rotor displacements and strains are calculated. Using a computer program the unbalance due to thermal effects is calculated and this result with the rotor neutral axis deformed shape is used as load in another finite element model that gives the rotor unbalance response. The methodology developed is applied in a 2-pole induction machine rotor in order to compare two different cage materials, aluminum and copper, under thermal bow point of view. It is concluded that the aluminum cages presents the same or even better performance regarding to vibration and thermal rotor bow, when compared to copper cages. Aluminum has the advantage of appling the rigid rotor concept to higher power outputs. This is a desirable characteristic for variable speed machines, where is required to avoid the rotor critical speed for the entire operating range The methodology can be extended to other rotary machinery where this effect is important to the overall vibration level in order to compare different designs and materials. It is suggested that the shaft design of the aluminum cage rotor can be changed in order to have its critical speeds close to the copper cage rotor ones. This will reduce the amplification factor of the aluminum cage rotor at operating speed, improving its performance.

Keywords*: Rotor thermal bow, Induction motors, Rotor dynamics*

1. Introduction

Material selection has been always an aim of discussion between engineers, especially when the material needs to meet several design requirements in different fields of technology. Material selection for the cage of an induction machine is a good example. Several authors like Finley and Hodowanec have analyzed induction motors material cage under manufacturing process point of view. Others like Dymond and Findlay analyzed material cage under application and reliability point of view. However, there is almost no published written work about an important customer request: vibration increase due to thermal effects.

Current thesis, of some users and manufactures of high speed induction motors, is that copper cage motors present enhanced behavior regarding to vibration and rotor thermal bow. This conclusion came from the fact that in general aluminum thermal expansion coefficient is higher than copper and its alloys. It is supposed that the aluminum cage would introduce bigger expansion forces in the rotor and as consequence would introduce higher rotor thermal shaft bow. However, this conclusion can be wrong, since it considers only the thermal expansion coefficient in the "analysis".

In order to properly evaluate which material is better under thermal rotor bow point of view, it is necessary to calculate the forces due to bars thermal expansion in the rotor, predict the rotor thermal bow and calculate the vibration vector for both configurations.

Using a simple analytical model, where the thermal expansion forces are calculated based on the material Young's modulus and its thermal expansion coefficient, it can be shown that aluminum cage will introduce smaller rotor bow due to thermal loading.

This analysis is quite simple and does not compare both rotor configurations dynamic response to introduced thermal rotor bow and unbalance. Using a finite element model of the rotor, the rotor thermal bow and the introduced unbalance are calculated for both configurations and then these results are used in another finite element model that calculates the rotor dynamic response.

2. The rotor of high speed induction machine

The rotor of a high speed induction machine can be divided in 3 main parts. The shaft, which is responsible to transmit the motor torque and where all the other components are assembled, the rotor core that is the main part in the magnetic circuit and the cage that is responsible to carry the induced current from one pole to another. Since the rotor is

part of the ventilation system of the machine, it has fans to induce pressure and flow and axial and radial ducts to distribute the air flow through the stator core. Figure 1 shows a cross section view of a 2-pole induction rotor.

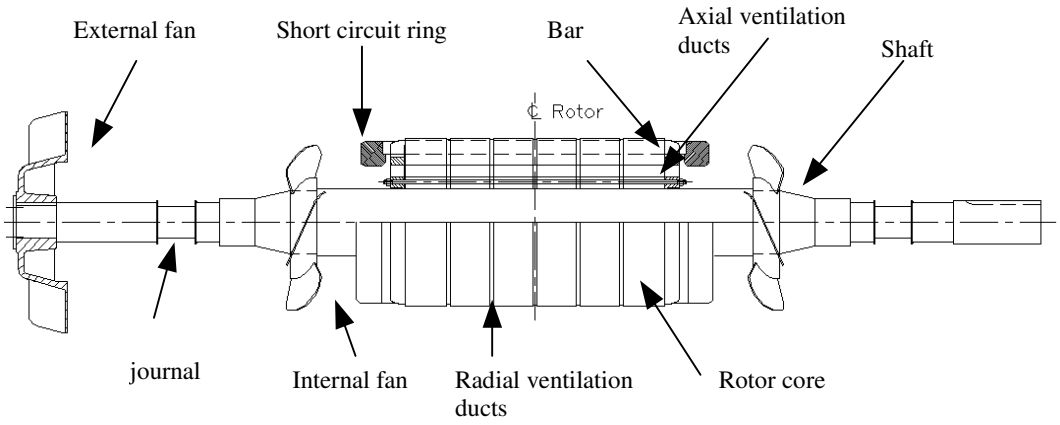

Figure 1: Longitudinal section view of a high speed induction rotor.

The induced current in the bars will generate Joule losses and the magnetic field in the core will generate magnetic core losses, being these responsible for rotor parts temperature increase. This temperature field distribution and the thermal unevenly expansion of the parts can bend the rotor and introduce bow and unbalance as function of temperature increase. This phenomenon is known as "thermal rotor bow" or "thermal vector", since the vibration amplitude and phase angle change as function of temperature.

Generally the core is kept tight by a rotor flange and axial studs in fabricated rotors. In cast rotors the cage is generally used also to keep the rotor core tight, since there is no rotor flange. The cast aluminum cage is the less expansive process while the fabricated cooper cage is the most expensive. In machines above 200 kW, cast rotors are usually aluminum, since copper cast involves a big investment, while fabricated rotors can be aluminum or copper.

The American Petroleum Institute Standard 541 defines acceptable limits for the vector change in vibration levels of squirrel cage induction motors. API 541 also almost requires fabricated copper rotors, since it establishes that cast or fabricated aluminum can be used if the vendor can demonstrate successful experience in starting duty requirements with a fatigue life of 5000 full voltage starts.

This paper compares both materials under thermal rotor bow point of view, assuming an aluminum inserted bar rotor, similar to the fabricated copper ones.

3. Models to evaluate rotor thermal bow

3.1. Analytical model

With the purpose of evaluating the rotor bars forces introduced due to temperature change of each bar material, let's take the rotor of figure 2, with the material properties of its bars and core defined.

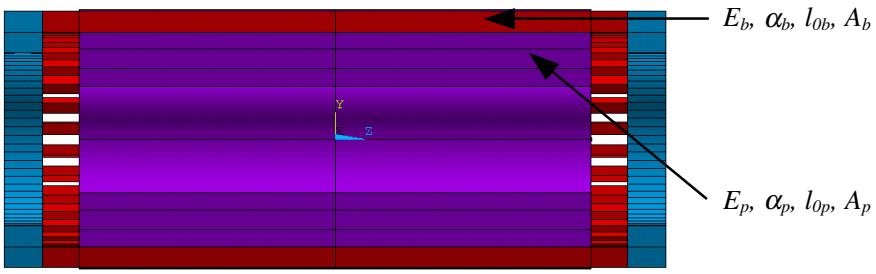

Figure 2 – Cross section of a squirrel cage induction motor rotor core.

Assuming the hypothesis that the deformations are significant only in the axial direction of the rotor, the thermal expansion force of one bar is given by the expression:

$$F_b = \frac{E_b * l_{0b} * \alpha_b * \Delta T_b * A_b}{l_{0b}} \tag{1}$$

Where A is the area (m^2), E is the Young's modulus (MPa), l is the length (m) and T is the temperature (°C). The subscripts identify: *al*, aluminum or its alloy; *b*, rotor bar; *cu*, copper or its alloys and *p,* rotor core. The Greek symbols means: α, thermal expansion coefficient ($°C^{-1}$); ν, Poisson's ratio; Δ, finite variation of one quantity and ρ is the material density (kg/m^3).

Taking Ap, as the area of rotor core around one bar, the thermal expansion force of that region of the rotor core is given by:

$$F_p = \frac{E_p * l_{0p} * \alpha_p * \Delta T_p * A_p}{l_{0p}} \tag{2}$$

Defining R_1, the ratio between F_b and F_p, for copper alloy bars and defining R_2 as the ration between F_b and F_p, for aluminum alloy bars, dividing R_1 per R_2 and reducing the redundant variables, we have:

$$\frac{R_1}{R_2} = \frac{E_{cu} * \alpha_{cu}}{E_{al} * \alpha_{al}} \tag{3}$$

This expression can be used to evaluate the ratio between the introduced forces due to thermal expansion of two different material bars. We can assume that this ratio will represent also the ratio of introduced thermal rotor bow.

3.2. Numerical model

The analytical model proposed in the previous section can be used to perform a qualitative analysis of different rotor bar materials, but does not take into account parameters such as rotor stiffness, bearing oil film changes due to different bearing loads and the change in critical speeds due to different rotor mass and inertia, that are affected by changing the overall rotor mass. In order to perform a more accurate analysis, keeping all the geometry variables constants and using only the bar material as a parameter, the following methodology is proposed:

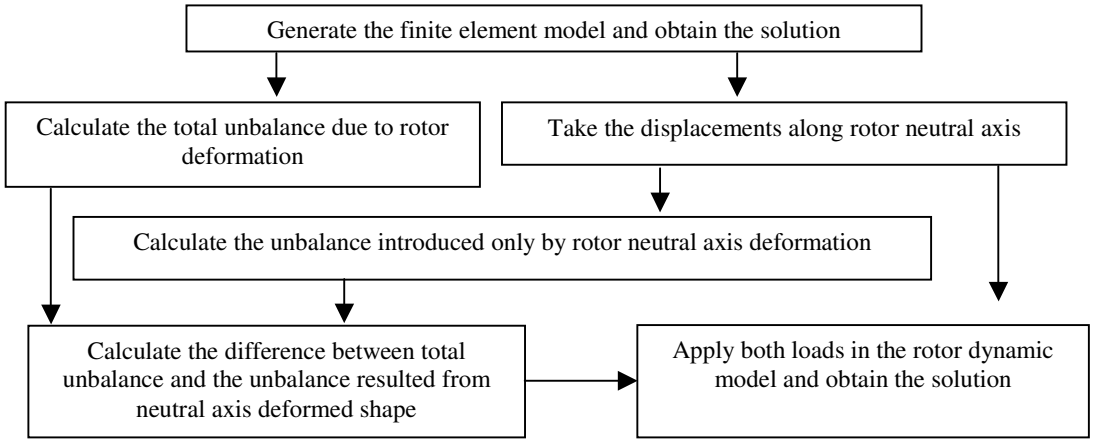

Figure 3 – Methodology proposed to evaluate the rotor dynamic response to thermal bow.

3.3. Material properties

The material properties considered in both analytical and numerical analysis are shown in Table 1. Values are for room temperature.

Table 1 – Material properties.

Component	Material	E (MPa)	ν	α (°C^{-1})	ρ (kg/m^3)
Bars	Copper alloy	96 000	0.32	1.75 10^{-5}	8510
	Aluminum alloy	70 700	0.33	1.69 10^{-5}	2720
Short circuit ring	Copper	116 700	0.33	1.70 10^{-5}	8910
	Aluminum alloy	70 700	0.33	1.69 10^{-5}	2720

The rotor core was represented as a solid structure with its stiffness properties represented by an orthotropic material as suggested by Wang and Lai.

3.4. Static analysis finite element model

Figure 4 shows the finite element model used in the linear static analysis that calculates the rotor bending and unbalance due to temperature increase in the rotor parts. All the rotor parts were modeled by 8-node solid elements. At the center of the bearing journals, spring elements with 0,001 times the stiffness of the shaft in the same direction. At the other node of these elements the boundary conditions were applied. This procedure was done in order to minimize the effect of the boundary conditions in the displacements of the rotor and avoid singularities in the stiffness matrix. Once it is assumed that there is no sliding between the components, coincident mesh was assumed between bars and core and between the rotor core and the shaft.

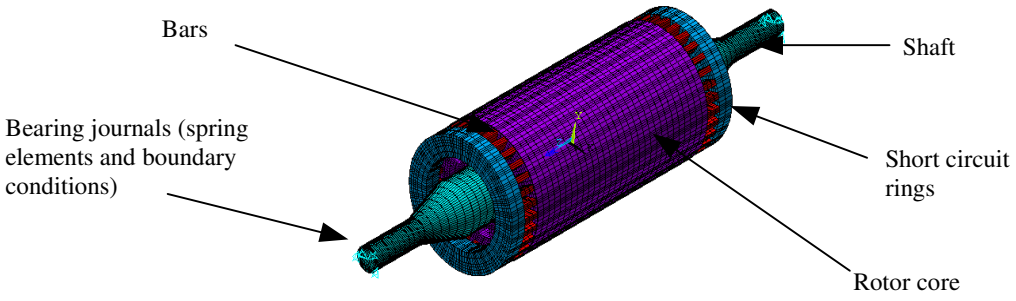

Figure 4 – Finite element model.

Finley and Hodowanec suggest that one of the possible causes of rotor thermal bow is due to uneven heating or cooling in the rotor bars. In order to compare both materials it was supposed that one quarter of the bars would present a temperature 85 °C while the rest of the bars would be at 80 °C. A temperature gradient was assumed for the rotor core, as show in figure 5. The shaft was assumed to have no temperature increase.

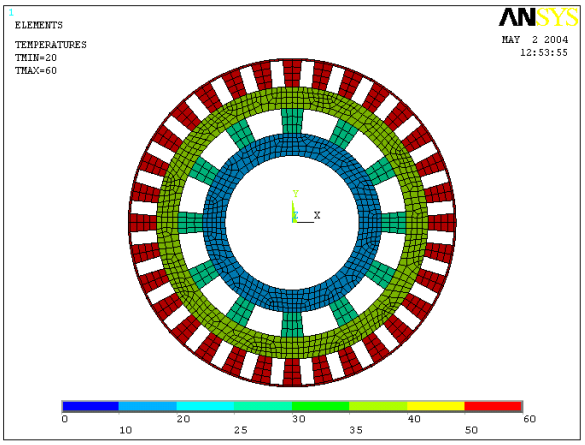

Figure 5 – Rotor core temperature gradient.

3.5. Rotor dynamics model

Figure 6 shows the rotor dynamic model used in the analysis that calculates rotor response to rotor bending and unbalance due to temperature increase in the rotor parts. Rotors are analyzed as a series of mass elements connected by beams, supported by multiple bearings, using the finite element method as suggested by Rao and following the lateral rotor dynamics analysis tutorial of API standard 684.

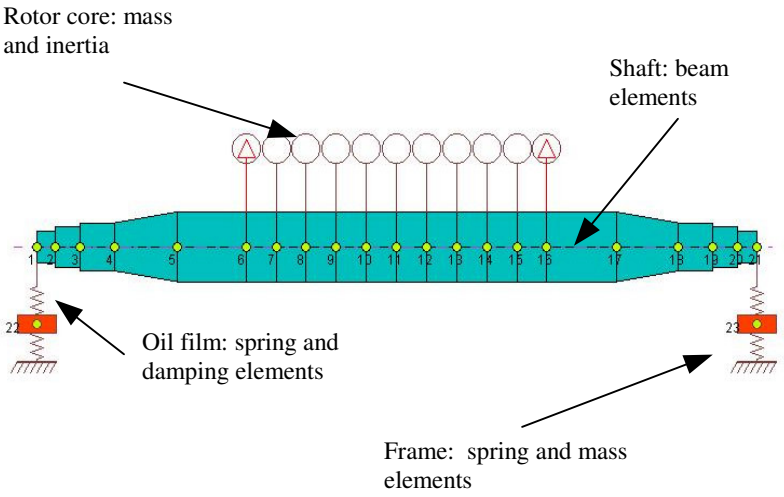

Figure 6 – Finite element model for dynamic analysis.

The shaft is represented by beam elements with stiffness, mass and inertia characteristics. The bearings are described by speed dependant cross-coupled linear stiffness and damping matrices. Flexible bearing supports with no damping also are considered in the analysis. These supports represent the equivalent stiffness of the bearing housing and the motor frame. The bearing housing and the bearing bracket masses are also represented in the nodes 22 and 23.

Rao suggests that a thermal bow can be modeled as an unbalance and Bachschmid, Pennacchi and Vania suggest that it can be modeled as two moments that will produce the same deformed shape. It was chosen to model the thermal bow using a combination the two suggested approaches, a rotor bow and a remaining unbalance.

4. Results

4.1. Analytical model

Using the values for E and α defined in table 1, considering copper alloy bars and aluminum bars, the ration between R_1 and R_2 is 1.40, what shows that the fabricated brass rotor bars should be 40% more sensitive to thermal bow than the fabricated aluminum rotor bars. Even if we assume the upper limit of 2.34 10-5 for the aluminum thermal expansion, the ratio is decreased to 1, what shows that there is no difference in thermal rotor bow between aluminum alloys and copper alloys cages.

4.2. Numerical models – Static analysis results

Figure 7 shows the rotor deformed shape for the copper alloy cage. The shaft neutral axis deflection is 0,032 mm in the mean line and the overall gravity center shift is 0,025 mm.

a) b)

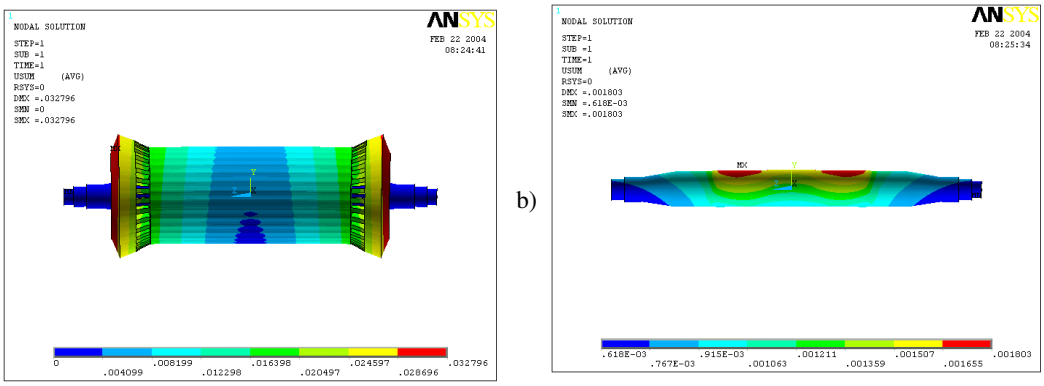

Figure 7 – a) Rotor deformations for the copper alloy bar rotor and b) shaft deformations, under proposed load case.

Figure 8 shows the rotor deformed shape for the aluminum alloy cage. In this case the shaft neutral axis deflection is 0,028 mm in the mean line and the overall gravity center shift is 0,023 mm. These values are 87,5 or 92% of the values calculated for the copper cage rotor, what shows that the aluminum cage introduces less rotor bow. However, once the shaft stiffness was kept constant and the rotor mass changes due to the difference in density of the two materials, the rotor dynamics will be different and is necessary to evaluate the dynamic response of both cases.

a) b)

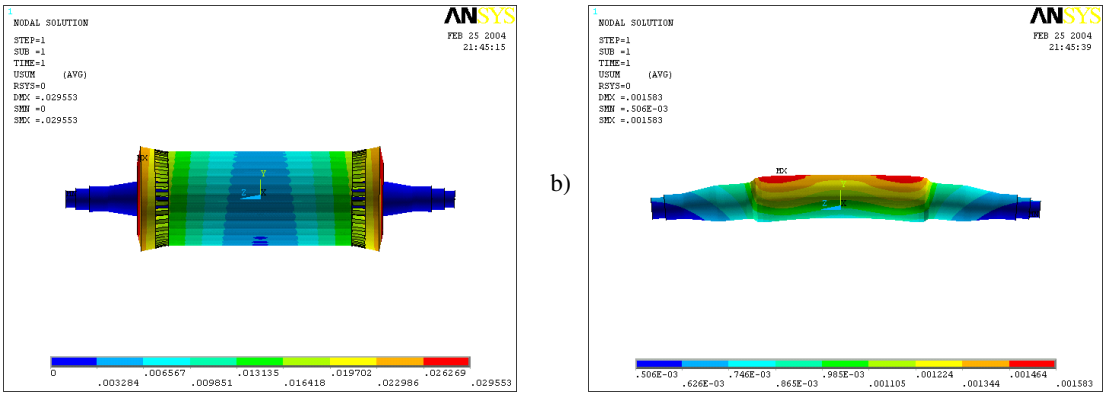

Figure 8 – a) Rotor deformations for the aluminum alloy bar rotor and b) shaft deformations, under proposed load case.

4.3. Numerical models – Rotor dynamics analysis results

Table 2 shows the total calculated unbalance, the total unbalance due to rotor neutral axis deformation and the remaining unbalance to be applied in the center of the rotor. It can be notice that the remaining unbalance is almost zero, but this can not be true when there is local heating or sliding between rotor parts, when the methodology proposed will produce more accurate results than introducing only the neutral axis deformed shape.

Table 2 – Calculated unbalance values for rotor dynamic analysis.

Rotor cage material	Total unbalance (g.mm)	Total unbalance due to rotor neutral axis bow (g.mm)	Remaining unbalance to be applied in the rotor (g.mm)
Copper alloy	24 272	25 000	-728
Aluminum alloy	19 000	18 863	137

In order to compare the introduced rotor bow effect in vibration levels, the unbalance level grade 6.3 as defined in ISO standard 1940-1 [7] was considered at cold condition. Table 3 shows the unbalance levels at the bearing journal node at critical speed and at rated speed for horizontal and vertical directions. Calculated critical speeds are 2180 rpm horizontal and 2590 rpm vertical for the copper alloy cage rotor and 2350 rpm horizontal and 2810 rpm vertical for the aluminum cage rotor. Figure 9 shows both rotor unbalance response analysis.

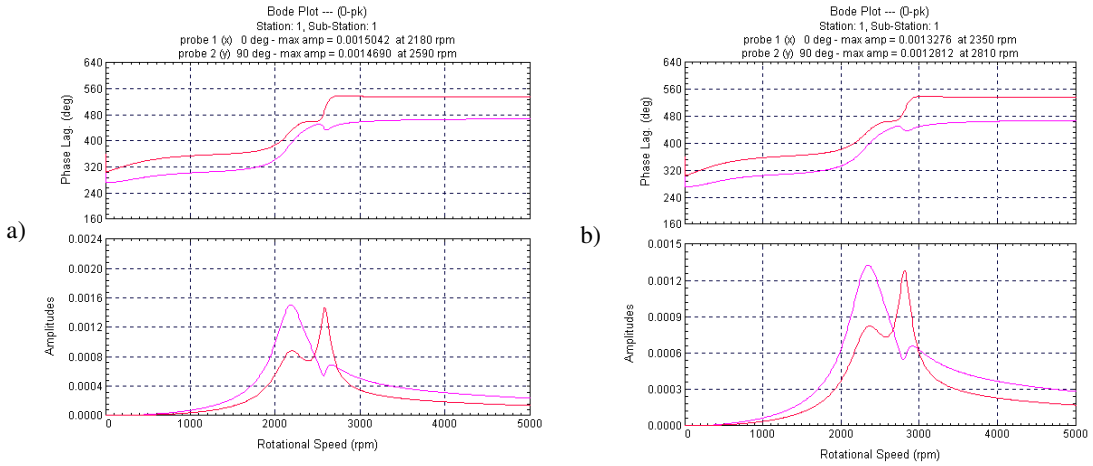

Figure 9 – Unbalance response analysis from 0 to 5000 rpm considering rotor with initial unbalance ISO grade 6.3. a) Copper cage rotor and b) Aluminum rotor.

Table 3 – Displacement values for both rotors of unbalance grade ISO 6.3.

Rotor cage material	Displacement at critical speed (μm)		Displacement at 3600 rpm (μm)	
	Horizontal	Vertical	Horizontal	Vertical
Copper alloy	38	37	9	6
Aluminum alloy	34	33	11	7

Table 4 shows the displacement levels at critical speeds and rated speed for the models where it was considered the shaft bow effect in phase with the initial rotor unbalance grade ISO 6.3. Figure 10 shows the rotor unbalance response analysis with initial unbalance ISO grade 6.3 plus the thermal rotor bow and unbalance.

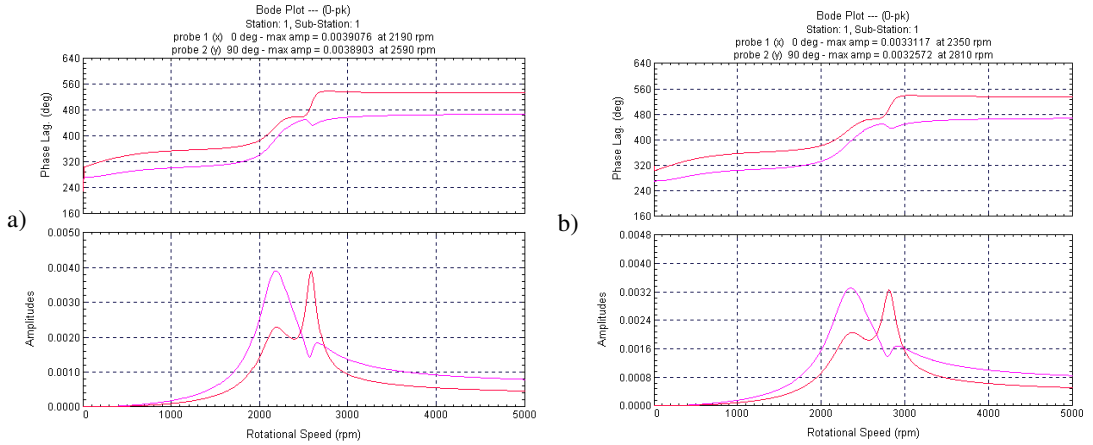

Figure 10 – Unbalance response analysis from 0 to 5000 rpm considering rotor with initial unbalance ISO grade 6.3 and rotor thermal bow. a) Copper cage rotor and b) Aluminum rotor.

Table 4 – Displacement values for both rotors of unbalance grade ISO 6.3 plus the rotor thermal bow and unbalance.

Rotor cage material	Displacement at critical speed (μm)		Displacement at 3600 rpm (μm)	
	Horizontal	Vertical	Horizontal	Vertical
Copper alloy	99	99	26	16
Aluminum alloy	84	83	29	19

5. Conclusions

The results of both rotors with initial unbalance ISO 6.3 are within the limits defined per API 541, being the predicted vibration values for the aluminum cage rotor slightly above the copper cage ones. However, this is not related to the cage material, but to the fact the once the stiffness of the shaft was kept constant, the critical speeds of the aluminum rotor are closer to the running speed, resulting in a higher amplification factor at rated speed.

It is suggested, as a further research, to introduce modifications in the shaft of the aluminum rotor, in order to have its critical speeds more close to the copper ones. Since it will reduce the amplification factor of the aluminum rotor at operating speed, its is expected the performance of this rotor can be improved, however the shaft bow will be higher since the rotor will be more flexible.

Vibration values calculated for both rotors, taking initial unbalance and thermal rotor bow are within the acceptable limits of API 541 as well as the vibration vector increase due to temperature as required by API 541.

It is concluded that if the same rotor construction is chosen, there is no such difference in vibration increase due to temperature if the cage material is a copper alloy or an aluminum alloy. The aluminum rotors present the advantage that the rigid rotor concept can be applied in a wider ranger of power outputs. Rigid rotor have the advantage of not presenting critical speeds in the hole operating range, being this a desirable characteristic in variable speed machines, as suggested by Owen.

6. Acknowledgements

The authors thanks to: GEVISA S/A to the information and tools provided to develop this research and to the professors Francisco Nigro and Demétrio C. Zachariadis per the suggestions in the modeling techniques.

7. References

API Standard 541 3rd Edition, 1995, “Form-Wound Squirrel Cage Motors – 250 Horsepower and Larger” Washington D.C, United States of America.

API Standard 684, 1st Edition, 1996, “Tutorial on the API Standard Paragraphs Covering Rotor Dynamics and Balancing: An Introduction to Lateral Critical and Train Torsional Analysis and Rotor Balancing” Washington D.C, United States of America.

Bachschmid, N.; Pennacchi, P.; Vania, A., 2002, “Indetification of Multiple Faults in Rotor Systems” Journal of Sound and Vibration, Vol. 254 (2) pg. 327-366.

Dymond, J. H. and Findlay, R. D., 1995, “Some Commentary on the choice of rotor bar material for induction motors” IEEE/PES Winter Meeting, New York, NY.

Finley, W. R.; Hodowanec, M. M. 2000, “Selection of Copper vs. Aluminum Rotors for Induction Motors” Petroleum and Chemical Industry Conference, p. 187-197, IEEE.

International Standard 1940-1, 1st Edition, 1986, “Mechanical vibration-Balance quality requirements of rigid rotors – Part 1: Determination of permissible residual unbalance”.

Owen, E. L., 1991, “Flexible Shaft Versus Rigid Shaft Electric Machines for Petroleum and Chemical Plants” IEEE Trans. Industry Applications, vol. 27 no 2.

Rao, J. S., 1996, “Rotor Dynamics” 3rd edition, New Age International (P) Ltd.

Wang, C.; Lai, C. S., 1999, “Vibration Analysis of an Induction Motor” Journal of Sound and Vibration, 224(4), pg. 733-756.

8. Responsibility notice

The authors are the only responsible for the printed material included in this paper.